


## Spin-1 glueballs in the Witten-Sakai-Sugimoto model

Florian Hechenberger<sup>✉</sup>, Josef Leutgeb<sup>✉</sup>, and Anton Rebhan<sup>✉</sup>

*Institut für Theoretische Physik, Technische Universität Wien,  
Wiedner Hauptstrasse 8-10, A-1040 Vienna, Austria*

 (Received 20 February 2024; accepted 29 February 2024; published 12 April 2024)

We consider the vector and the pseudovector glueball in the top-down holographic model of large- $N_c$  QCD of Witten and their decays into ordinary mesons described by the D8 brane construction due to Sakai and Sugimoto. At leading order, the relevant interactions are determined exclusively by the Chern-Simons action of the D8 branes and are thus rigidly connected to the chiral anomaly and the Wess-Zumino-Witten terms. As found in a previous study of the pseudovector glueball, which we revisit and complete, the resulting decay widths are surprisingly large, implying that both the pseudovector and the vector glueball are very broad resonances, with a conspicuous dominance of decays into  $a_1\rho$  and  $K_1(1400)K^*$  in the case of the vector glueball. We also obtain a certain weak mixing of vector glueballs with ordinary vector mesons, but we conclude that it does not provide an explanation for the so-called  $\rho\pi$  puzzle in charmonium decays.

DOI: [10.1103/PhysRevD.109.074014](https://doi.org/10.1103/PhysRevD.109.074014)

### I. INTRODUCTION AND SUMMARY

In spite of extensive theoretical and experimental studies, the status of glueballs in the hadron spectrum of QCD remains largely unsettled [1–4]. While the spectrum of glueballs as obtained in lattice QCD [5–9] appears to be relatively stable when dynamical quarks are included, their interactions and the amount of mixing with ordinary mesons are difficult to pin down, so that no clear glueball state could be identified yet.

Lattice QCD indicates that the lightest glueball is a  $J^{PC} = 0^{++}$  scalar with a mass between 1500 and 1800 MeV, but phenomenological studies disagree [10–16] whether to identify it as a smaller or larger component of the scalar-isoscalar mesons  $f_0(1500)$ ,  $f_0(1710)$ , or a novel  $f_0(1770)$ , or instead as a wide resonance distributed over several scalars [17].

The next lightest glueball is the  $2^{++}$  tensor glueball associated with the Pomeron [18], where lattice QCD indicates a mass around 2400 MeV, while Pomeron physics favors a somewhat smaller mass, followed by the  $0^{-+}$  pseudoscalar around 2600 MeV, which is expected to play a role in the chiral anomaly and the large  $\eta'$  mass.

In this work we continue the studies of Refs. [19–25] using the Witten-Sakai-Sugimoto (WSS) model [26,27] to derive predictions for the interactions of glueballs with ordinary mesons as well as their radiative decays. The

Witten model [28] for low-energy large- $N_c$  QCD is based on a supersymmetry breaking background geometry provided by an  $N_c \gg 1$  stack of circle compactified D4 branes in type-IIA supergravity, and it has a spectrum of spin- $0^{\pm\pm}$ , spin- $1^{\pm-}$ , and spin- $2^{++}$  glueballs with a mass hierarchy that is qualitatively in agreement with lattice findings [29,30]. By adding stacks of  $N_f \ll N_c$  D8 and anti-D8 probe branes, Sakai and Sugimoto have succeeded in constructing a top-down holographic model that provides a geometric model of non-Abelian chiral symmetry breaking and reproduces numerous features of actual low-energy QCD qualitatively as well as semi-quantitatively, typically with 10%–30% deviations, with a minimal number of free parameters. Because no further free parameters are involved to determine the interactions with glueballs, the WSS model is also very predictive with respect to interactions between glueballs and ordinary mesons, which are treated as (approximately) unmixed in the 't Hooft limit  $g^2N_c \gg 1$ ,  $N_f \ll N_c$ , corresponding to a quenched approximation when we set  $N_f = N_c = 3$  in the end.

In Ref. [25] we have recently revisited the predictions of the WSS model for meson decays upon including the  $\eta'$  mass from the  $U(1)_A$  anomaly and adding a mass term for pseudoscalars induced by quark masses. Besides extending the decay patterns of scalar and tensor glueballs by radiative decay modes, we have also considered the pseudoscalar glueball, which is represented by a Ramond-Ramond 1-form field and whose interactions are determined by its anomaly-driven mixing with the  $\eta_0$  meson. The interactions of the latter are uniquely given by the Chern-Simons (CS) term of the flavor branes, hence completely determined by the anomaly structure.

---

*Published by the American Physical Society under the terms of the Creative Commons Attribution 4.0 International license. Further distribution of this work must maintain attribution to the author(s) and the published article's title, journal citation, and DOI. Funded by SCOAP<sup>3</sup>.*

In this paper, we extend the analysis to spin-1 glueballs, where the quenched lattice QCD simulation of Ref. [7] predicts masses around 3000 MeV for the pseudovector ( $1^{+-}$ ) and around 3800 MeV for the vector ( $1^{--}$ ) glueball, which is reproduced well by the WSS model as far as their ratio is concerned, while the overall scale is underestimated by about 30%. In the WSS model, the two spin-1 glueballs are represented by the Kalb-Ramond tensor field in conjunction with a Ramond-Ramond 3-form field. Their interactions with ordinary mesons are dominated by the unique CS action of the D8 branes; they are thus tied to the structure of the anomalous interactions of ordinary mesons. Moreover, through the Kalb-Ramond field, the  $1^{--}$  vector glueball mixes with the singlet component of ordinary vector mesons, which is interesting with regard to the proposal [31–33] that mixing with vector glueballs could explain the so-called  $\rho\pi$  puzzle in charmonium decays [34], which consists of a surprisingly strong suppression of  $\rho\pi$  and  $K^*K$  in the decay of  $\psi(2S)$  compared to  $\psi(1S) = J/\psi$ . However, in the WSS model the decay pattern of the vector glueball turns out to have a strong enhancement in the  $a_1\rho$ ,  $K_1K^*$ , and  $f_1\omega$  channels, which are not seen in any of the  $\psi(nS)$  decays. The results of the WSS model thus do not support an explanation of the charmonium  $\rho\pi$  puzzle through vector glueball admixtures.

The couplings and decay patterns of vector and pseudovector glueballs are also of interest with regard to the physics of the Odderon [18,35], which recently has been claimed to have been discovered in joint experiments by the TOTEM and D0 collaborations [36]. Brower *et al.* [37] have argued that in holographic QCD Odderons appear naturally as the Reggeized Kalb-Ramond modes in the Neveu-Schwarz sector of closed string theory, which contains both vector and pseudovector glueball modes whose interactions with ordinary hadrons are fixed in the WSS model without any additional free parameters.

However, as found in the previous study of the decays of the pseudovector glueball in Ref. [23], which we revisit and complete, the decay widths obtained in the WSS model are very large, making both spin-1 glueballs difficult to discover, albeit the peculiar decay pattern of the vector glueball may be helpful in this respect.

This paper is organized as follows. In Sec. II we recapitulate the WSS model as used in [25], but expanded to include all form fields relevant for spin-1 glueballs. In Sec. III we derive the bulk mode function of the vector glueball and describe its effects on the hadronic modes on the flavor branes, followed by a systematic evaluation of the hadronic and radiative decay modes, closing with a discussion of the implications for the  $\rho\pi$  puzzle in  $J/\psi$  and  $\psi'$  decays. In Sec. IV, we consider the pseudovector glueball, revisiting and completing the previous work of Ref. [23]. Section V contains our conclusions and comments on phenomenological consequences.

## II. QUICK REVIEW OF THE WITTEN-SAKAI-SUGIMOTO MODEL

The 10-dimensional background geometry corresponding to an  $N_c \gg 1$  stack of D4 branes compactified with supersymmetry breaking boundary conditions in the circular fourth spatial coordinate  $x^4 \equiv \tau$ ,

$$\tau \simeq \tau + \delta\tau = \tau + 2\pi M_{\text{KK}}^{-1}, \quad (2.1)$$

is given by the metric

$$\begin{aligned} ds^2 &= \left(\frac{U}{R_{\text{D4}}}\right)^{3/2} [\eta_{\mu\nu} dx^\mu dx^\nu + f(U) d\tau^2] \\ &\quad + \left(\frac{R_{\text{D4}}}{U}\right)^{3/2} \left[ \frac{dU^2}{f(U)} + U^2 d\Omega_4^2 \right], \\ e^\phi &= g_s \left(\frac{U}{R_{\text{D4}}}\right)^{3/4}, \quad F_4 = dC_3 = \frac{(2\pi l_s)^3 N_c}{V_4} \epsilon_4, \\ f(U) &= 1 - \frac{U_{\text{KK}}^3}{U^3}, \end{aligned} \quad (2.2)$$

with dilaton  $\phi$  and Ramond-Ramond three-form field<sup>1</sup>  $C_3$ . Here  $x^\mu$ ,  $\mu = 0, 1, 2, 3$ , are the coordinates in the flat four-dimensional directions,  $U$  is the radial holographic direction, where regularity at  $U = U_{\text{KK}}$  fixes

$$M_{\text{KK}} = \frac{3 U_{\text{KK}}^{1/2}}{2 R_{\text{D4}}^{3/2}}; \quad (2.3)$$

the radius  $R_{\text{D4}}$  is related to the string coupling  $g_s$  and the string length  $l_s$  through  $R_{\text{D4}}^3 = \pi g_s N_c l_s^3$ , and the 't Hooft coupling of the dual four-dimensional Yang-Mills theory that arises after Kaluza-Klein reduction is given by

$$\lambda = g_{\text{YM}}^2 N_c = \frac{g_s^2}{\delta\tau} N_c = 2\pi g_s l_s M_{\text{KK}} N_c. \quad (2.4)$$

This is a solution in type IIA supergravity, whose bosonic part reads [38]

$$\begin{aligned} S_{\text{IIA}} &= S_{\text{NS}} + S_R + S_{\text{CS}}, \\ S_{\text{NS}} &= \frac{1}{2\kappa_{10}^2} \int d^{10}x \sqrt{-g} e^{-2\phi} \left( R + 4\nabla_M \phi \nabla^M \phi - \frac{1}{2} |H_3|^2 \right), \\ S_R &= \frac{1}{2\kappa_{10}^2} \int d^{10}x \sqrt{-g} \left( -\frac{1}{2} |F_2|^2 - \frac{1}{2} |\tilde{F}_4|^2 \right), \\ S_{\text{CS}} &= -\frac{1}{2\kappa_{10}^2} \int d^{10}x \frac{1}{2} B_2 \wedge F_4 \wedge F_4, \end{aligned} \quad (2.5)$$

<sup>1</sup>Using standard string-theory conventions [38] for the normalization of Ramond-Ramond fields rather than the rescaled version of Ref. [26].

where

$$\begin{aligned} F_2 &= dC_1, & F_4 &= dC_3, \\ \tilde{F}_4 &= F_4 - C_1 \wedge H_3, & H_3 &= dB_2. \end{aligned} \quad (2.6)$$

The probe ( $N_f \ll N_c$ ) D8 and  $\overline{\text{D8}}$ -branes extend along  $x^\mu$ ,  $U$ ,  $S^4$  and are located in an antipodal configuration on the  $\tau$ -circle, joining smoothly at  $U_{\text{KK}}$ , thereby realizing spontaneous  $U_L(N_f) \times U_R(N_f)$  breaking.

The action for the flavor D8-branes is given by the sum of the DBI action and the Chern-Simons action

$$\begin{aligned} S_{\text{DBI}}^{\text{D8}} &= -T_8 \int d^9x \sqrt{-\det(g_{MN} + 2\pi\alpha' F_{MN} + B_{MN})}, \\ S_{\text{CS}}^{\text{D8}} &= T_8 \sum_p \int_{\text{D8}} \sqrt{\hat{A}(\mathcal{R})} \text{Tr} \exp(2\pi\alpha' F + B) \wedge C_p, \end{aligned} \quad (2.7)$$

with  $F$  the non-Abelian flavor field strength and  $\hat{A}(\mathcal{R})$  being the A-roof genus [38,39]. The sum in the Chern-Simons term is a formal sum over the p-form gauge fields in the Ramond-Ramond sector of the theory.

Following [26,27], the spectrum on the joined D8 and  $\overline{\text{D8}}$ -brane is truncated to include only  $SO(5)$  invariant states. To this end, and to quadratic order, the DBI action in Eq. (2.8) reduces to<sup>2</sup>

$$S_{\text{DBI}}^{\text{D8}} = -\kappa \int d^4x dz \text{Tr} \left[ \frac{1}{2} K^{-1/3} F_{\mu\nu}^2 + M_{\text{KK}}^2 K F_{\mu z}^2 \right], \quad (2.8)$$

with

$$\kappa \equiv \frac{\lambda N_c}{216\pi^3}, \quad K(z) \equiv 1 + z^2 = U^3/U_{\text{KK}}^3, \quad (2.9)$$

where  $z$  runs from  $-\infty$  to  $+\infty$  along the joined D8 branes.

Performing a Kalzua-Klein (KK) decomposition for the five-dimensional flavor gauge fields

$$\begin{aligned} A_\mu(x^\mu, z) &= \sum_{n=1}^{\infty} B_\mu^{(n)}(x^\mu) \psi_n(z) \\ A_z(x^\mu, z) &= \sum_{n=0}^{\infty} \varphi^{(n)}(x^\mu) \phi_n(z), \end{aligned} \quad (2.10)$$

yields a tower of massive vector and axial vector mesons corresponding to odd and even mode numbers  $n$  with even and odd  $z$ -parity, respectively (see our previous paper [25] for further details):

<sup>2</sup>Note that in (2.8) one uses the Minkowski metric  $\eta_{\mu\nu}$ , in the mostly plus convention, to contract the four-dimensional space-time indices.

$$v_\mu^n \equiv B_\mu^{(2n-1)}, \quad a_\mu^n \equiv B_\mu^{(2n)}, \quad (2.11)$$

Identifying the lightest vector mode with the  $\rho$  meson fixes  $M_{\text{KK}} = 949$  MeV [26,27], corresponding to  $m_\rho = 776.4$  MeV.

The scalar fields  $\varphi^{(n)}$  can be absorbed by the fields  $B_\mu^{(n)}$  except for  $\varphi^{(0)}$  which corresponds to the massless pseudo-scalar Goldstone multiplet of the broken chiral symmetry,

$$U(x) = e^{i\text{Tr}(\lambda^a \varphi^{(0)} T^a / f_\pi)} = \text{P exp } i \int_{-\infty}^{\infty} dz A_z(z, x), \quad (2.12)$$

with the Gell-Mann matrices  $\lambda^a = 2T^a$  and including the singlet term  $\lambda^0 = \sqrt{2/N_f} \mathbf{1}$ .

To fix the 't Hooft coupling  $\lambda$  we use the resulting pion decay constant

$$f_\pi^2 = \frac{\lambda N_c M_{\text{KK}}^2}{54\pi^4} \quad (2.13)$$

to get  $\lambda \approx 16.63$  from  $f_\pi \approx 92.4$  MeV. To obtain an error estimate and following [20] we shall also consider the smaller value  $\lambda \approx 12.55$  obtained by matching the large- $N_c$  lattice result for the string tension obtained in Ref. [40].

The non-normalizable modes of the flavor gauge field  $A_\mu$  can be used to introduce the photon field as an external source via [27]

$$\lim_{z \rightarrow \pm\infty} A_\mu(x, z) = A_{L,R\mu}(x) = eQ A_\mu^{\text{em}}(x), \quad (2.14)$$

with the quark charge matrix  $Q$  for  $N_f = 3$  given by

$$Q = \frac{1}{3} \begin{pmatrix} 2 & & \\ & -1 & \\ & & -1 \end{pmatrix}, \quad (2.15)$$

where  $e$  is the electromagnetic charge. As reviewed in our previous paper [25], vector meson dominance (VMD) arises because the photon field couples exclusively through mixing with the tower of vector mesons. For on-shell photons, the corresponding holographic wave function entering the overlap integrals with the mode functions of hadronic fields reduces to unity; off-shell photons involve nontrivial bulk-to-boundary propagators.

For  $N_f = 3$ , which we shall consider in the following, we also take into account that in the WSS model the  $U(1)_A$  flavor symmetry is broken by an anomalous contribution of order  $1/N_c$  due to the  $C_1$  Ramond-Ramond field, which gives rise to a Witten-Veneziano [41,42] mass term for the singlet  $\eta_0$  pseudoscalar with [24,26]

$$m_0^2 = \frac{N_f}{27\pi^2 N_c} \lambda^2 M_{\text{KK}}^2. \quad (2.16)$$

For  $N_f = N_c = 3$ , one has  $m_0 = 967\dots730$  MeV for  $\lambda = 16.63\dots12.55$ , which is indeed a phenomenologically interesting ballpark when finite quark masses are added to the model by the addition of an effective Lagrangian

$$\begin{aligned} \mathcal{L}_m^M &\propto \text{Tr}(MU(x) + \text{H.c.}), \\ M &= \text{diag}(m_u, m_d, m_s), \end{aligned} \quad (2.17)$$

which can be motivated by either world sheet instantons [43,44] or non-normalizable modes of additional bifundamental fields corresponding to open-string tachyons [45–48].

Assuming for simplicity isospin symmetry,  $m_u = m_d = \hat{m}$ , this leads to masses [22,25]  $m_\eta \approx 520\dots470$ ,  $m_{\eta'} \approx 1080\dots890$  MeV and mixing angles  $\theta_P \approx -14^\circ \dots -24^\circ$  for  $\lambda = 16.63\dots12.55$ .

In the following we shall consider this range of mixing angles in conjunction with the variation of  $\lambda$ , but we shall fix  $m_\eta$  and  $m_{\eta'}$  to their experimental values when evaluating phase space integrals.

Vector mesons remain unchanged by this introduction of quark masses. In the following we shall keep the (chiral) results for their couplings, but we will raise the masses of  $\omega$  and  $\phi$  mesons to their experimental values in phase space integrals, assuming ideal mixing.

In the WSS model, the axial vector meson  $a_1$  is predicted with mass 1186.5 MeV, very close to the experimental result of 1230(40) MeV. For the remaining axial vector mesons we again keep the chiral results for their couplings, but introduce phenomenological masses and mixing angles in phase space integrals. Here we use a mixing angle of  $\theta_f = 20.4^\circ$  for  $f_1$  and  $f'_1$  mesons in

$$\begin{aligned} |f_1(1285)\rangle &= \cos\theta_f |\bar{n}n\rangle - \sin\theta_f |\bar{s}s\rangle, \\ |f_1(1420)\rangle &= \sin\theta_f |\bar{n}n\rangle + \cos\theta_f |\bar{s}s\rangle. \end{aligned} \quad (2.18)$$

The physical strange axial vector mesons  $K_1(1270)$  and  $K_1(1400)$  are mixtures of  $K_{1A}$  ( $1^{++}$ ) and the excited axial vector meson  $K_{1B}$  ( $1^{+-}$ ) [49]. Because in the WSS model, there is no  $1^{+-}$  nonet of ordinary mesons, only  $K_{1A}$  is present, which couples to the physical  $K_1$  mesons according to their mixing defined by

$$|K_{1A}\rangle = \cos\theta_K |K_1(1400)\rangle + \sin\theta_K |K_1(1270)\rangle. \quad (2.19)$$

In [49,50] the favored mixing angle is quoted as  $|\theta_K| \approx 33^\circ$ , which we adopt in the following.

Encouragingly, the WSS model predicts rather well the ballpark of several hadronic decays such as  $\rho \rightarrow \pi\pi$ ,  $\omega \rightarrow \pi\pi\pi$ ,  $a_1 \rightarrow \rho\pi$ , and also various radiative decays, see Refs. [20,25–27].

### III. THE VECTOR GLUEBALL IN THE WSS

The mass spectra for the spin-1 fluctuations in the M-theory lift of the Witten model were first obtained in [30] by considering the fluctuations of  $A_{MNO}$  and  $A_{MN11}$ . In the 10D string frame, these fluctuations translate to  $C_3$  and  $B_2$ , respectively.

Treating contributions stemming from the D8-branes as perturbations later on, the relevant field equations are obtained by varying Eq. (2.5) with respect to  $B_2$  and  $C_3$

$$\begin{aligned} \nabla_O(e^{-2\phi} H^{OMN}) \\ - \frac{1}{2! \cdot (4!)^2 \sqrt{-g}} \epsilon^{MNO_1\dots O_8} F_{O_1\dots O_4} F_{O_5\dots O_8} &= 0, \\ \nabla_P F^{PMNO} \\ - \frac{1}{3! \cdot 4! \sqrt{-g}} \epsilon^{MNOP_1\dots P_7} H_{P_1 P_2 P_3} F_{P_4\dots P_7} &= 0. \end{aligned} \quad (3.1)$$

#### A. Ansatz, normalization, and equations of motion

In [30] the  $1^{--}$  vector glueball mode is obtained from the  $A_{\mu\nu\tau}$  and  $A_{\mu r 11}$  components of the 11D gauge field  $A_3$  which translates to  $C_{\mu\nu\tau}$  and  $B_{\mu u}$  in the 10D string frame. Note that including the  $B_{\mu u}$  fluctuation is necessary to obtain a consistent solution of the equation of motion since these two fluctuations are tied by a topological mass term. Starting from the ansatz

$$\begin{aligned} C_{\mu\nu\tau} &= \frac{a(u)}{g_s} \tilde{C}_{\mu\nu}(x^\mu), \\ B_{\mu u} &= \frac{3}{2\Box} \frac{u^2}{u^3 - 1} a(u) \eta_{\mu\kappa} \epsilon^{\kappa\nu\rho\sigma} \partial_\nu \tilde{C}_{\rho\sigma}(x^\mu), \end{aligned} \quad (3.2)$$

and neglecting backreactions from the DBI action, we obtain the mode equation for the vector glueball

$$\begin{aligned} a''(u) + a'(u)/u + a(u) \left( M^2 \frac{R^3}{U_{\text{KK}}(u^3 - 1)} - \frac{9u}{u^3 - 1} \right) &= 0, \\ u &= U/U_{\text{KK}}. \end{aligned} \quad (3.3)$$

The relation to the notation used in [30] is

$$a(u) = \sqrt{r^6/r_{\text{KK}}^6 - 1} M_4(r), \quad u^3 = r^6/r_{\text{KK}}^6, \quad (3.4)$$

and when using coordinates  $z$  along the D8 branes we have  $a(z) = z M_4(z)$ .

By imposing the boundary conditions  $M'_4(U_{\text{KK}}) = 1$  and  $M_4(\infty) = 0$  we obtain the mass spectrum  $M_V^2 = \lambda_V M_{\text{KK}}^2$  with the first three eigenvalues given by  $\lambda_V = \{9.22721, 15.9535, 24.1552\}$ . The lowest eigenvalue corresponds to the mass of  $M_V = 2883$  MeV which is below the (quenched) lattice result of  $\approx 3850$  MeV [6,7].

To fix the normalization we induce the fluctuations (3.2) in (2.5) and utilize the equation of motion (3.3) to get

$$\mathcal{L}_V^{(2)} = -\frac{1}{2\kappa_{10}^2} \frac{1}{4g_s^2} \frac{R^6}{U_{\text{KK}}} \sqrt{\hat{g}_{S_4}} \frac{u}{u^3-1} a(u)^2 \tilde{C}_{\mu\nu} (M^2 - \square) \tilde{C}_{\mu\nu}. \quad (3.5)$$

Requiring a kinetic term with canonical normalization after integrating over the holographic coordinate, the  $S_4$ , and the  $S_1$ , we set  $a(u) \rightarrow a(u)/\mathcal{N}_V$  with

$$\int du \frac{1}{2\kappa_{10}^2} \frac{2\pi}{M_{\text{KK}}} V_4 \frac{R^6}{U_{\text{KK}} g_s^2} \frac{u}{u^3-1} \mathcal{N}_V^{-2} a(u)^2 = 1, \quad (3.6)$$

leading to

$$\mathcal{N}_V^2 = \frac{3}{16} \frac{\lambda N_c^2}{(2\pi)^2 M_{\text{KK}}^4 R^6} \int_1^\infty du u M_4(u)^2, \quad u = \frac{U}{U_{\text{KK}}}, \quad (3.7)$$

with

$$\mathcal{N}_V = 0.0142218 \frac{\sqrt{\lambda} N_c}{M_{\text{KK}}^2 R^3} \quad (3.8)$$

for the ground-state vector glueball.

When considering interactions with modes on the flavor branes, the integration variable  $z$  covers the holographic radial coordinate twice. The glueball modes are all even under  $z$ -parity. However the rescaling employed above corresponds to  $a(z) = z M_4(z)$  and thus  $M_4(z)$  has odd parity on the joint flavor branes.

## B. Bilinear corrections due to the DBI action

Because the Kalb-Ramond field couples directly to the flavor branes through the DBI action, the latter gives rise to bilinear terms involving the vector glueball field and the singlet component of the vector meson field.

### 1. Mass correction

Integrating over the holographic direction and the  $S^4$ , the DBI action gives rise to an additional mass term for the vector glueball proportional to  $N_f/N_c$ , given by

$$\begin{aligned} S_{\text{DBI}} &= -T_8 \text{tr} \int d^9 x e^{-\phi} \sqrt{-g_{MN} + (2\pi\alpha') F_{MN} + B_{MN}} \\ &\supset -T_8 N_f \left( \frac{8\pi^2}{3} \right) \int d^4 x dz \sqrt{-g_{D8}} e^{-\phi} \frac{1}{2} g^{\mu\nu} g^{zz} B_{\mu z} B_{\nu z} \\ &= -\frac{2\lambda^3 N_f N_c}{27(2\pi)^5 R^6} \int d^4 x dz (1+z^2) M_4(z)^2 \frac{1}{2\square} \eta^{\mu\nu} V_\mu V_\nu \\ &= -\int d^4 x \frac{1}{2} \delta\lambda_V M_{\text{KK}}^2 \eta^{\mu\nu} V_\mu V_\nu, \\ \delta\lambda_V &= \frac{2\lambda^3 N_f N_c}{27(2\pi)^5 M_{\text{KK}}^2 R^6 M_V^2} \int dz (1+z^2) M_4(z)^2 \\ &= 0.00233\lambda^2 \frac{N_f}{N_c} \end{aligned} \quad (3.9)$$

where we projected out the spin-1 part of  $\tilde{C}_{\rho\sigma}(x^\mu)$  with  $\tilde{C}_{\rho\sigma}(x^\mu) = \frac{1}{\sqrt{\square}} \epsilon_{\rho\sigma}{}^{\kappa\lambda} \partial_\kappa V_\lambda(x^\mu)$ . Treating this contribution perturbatively we obtain for  $N_f = 3, N_c = 3, \lambda = 16.63\dots 12.55$  an increase of the mass of the vector glueball of  $100\dots 57$  MeV, i.e., only  $3.4\dots 2\%$ .

Since this correction is of the same order as backreaction effects [51,52] that we otherwise ignore in the following,<sup>3</sup> and since it is numerically quite negligible, we shall later use only the leading order result for the vector glueball mass.

### 2. Mixing with vector mesons

A parametrically more important term of order  $\sqrt{N_f/N_c}$  is given by a bilinear term involving the vector glueball and the singlet flavor gauge field  $\hat{v} = v^{a=0}$ . Explicitly it is given by

$$\begin{aligned} S_{\text{DBI}} &= -T_8 \text{tr} \int d^9 x e^{-\phi} \sqrt{-g_{MN} + (2\pi\alpha') F_{MN} + B_{MN}} \\ &\supset -\int d^4 x \xi_n \eta^{\mu\nu} \hat{v}_\mu^n(x^\mu) V_\nu(x^\mu), \\ \xi_n &= \frac{\kappa\lambda}{2\pi M_V} \frac{M_{\text{KK}}}{R^3} \text{tr} T^0 \int dz (1+z^2) M_4(z) \psi'_{2n-1}(z) \\ &= \{-0.0180, -0.0165, 0.005, \dots\} \lambda M_{\text{KK}}^2 \sqrt{\frac{N_f}{N_c}} \end{aligned} \quad (3.10)$$

for the first three vector meson modes. Note that, as explained above, the integral over  $z$  involves  $M_4$  as an odd function. Restricting to the ground-state singlet vector meson, the combined kinetic terms for singlet vector mesons and the vector glueball are then given by a

$$\begin{aligned} \mathcal{L}_{V,\hat{v}}^{(2)} &= -\int d^4 x \left( \frac{1}{4} \hat{f}_{\mu\nu}^2 + \frac{1}{2} m^2 \eta^{\mu\nu} \hat{v}_\mu \hat{v}_\nu + \xi_1 \eta^{\mu\nu} \hat{v}_\mu V_\nu \right. \\ &\quad \left. + \frac{1}{4} (F_{\mu\nu}^V)^2 + \frac{1}{2} M_V^2 \eta^{\mu\nu} V_\mu V_\nu \right). \end{aligned} \quad (3.11)$$

With degenerate vector meson masses, the Lagrangian is readily diagonalized by a unitary field redefinition

$$\begin{aligned} V_\mu &\rightarrow \tilde{V}_\mu \cos \theta - \tilde{v}_\mu \sin \theta \\ \hat{v}_\mu &\rightarrow \tilde{V}_\mu \sin \theta + \tilde{v}_\mu \cos \theta \end{aligned} \quad (3.12)$$

with mixing angle

$$\theta = \frac{1}{2} \arctan \frac{2\xi_1}{M_V^2 - m^2} \quad (3.13)$$

and masses

<sup>3</sup>See Ref. [53] for a recent study of such backreaction effects for the glueballs of the WSS model.

$$\begin{aligned}\tilde{m}^2 &= m^2 \left( \cos^2 \theta + \frac{M_V^2}{m^2} \sin^2 \theta - \frac{2\xi_1}{m^2} \sin \theta \cos \theta \right), \\ \tilde{M}_V^2 &= M_V^2 \left( \cos^2 \theta + \frac{m^2}{M_V^2} \sin^2 \theta + \frac{2\xi_1}{M_V^2} \sin \theta \cos \theta \right).\end{aligned}\quad (3.14)$$

For example, for  $N_f = 2$ , where  $\rho$  and  $\omega$  are approximately degenerate, we obtain

$$\theta = -(1.52\dots 1.18)^\circ \quad (3.15)$$

with  $M_V = \sqrt{\lambda_V + \delta\lambda_V} M_{\text{KK}} = (2949\dots 2921)$  MeV. After the diagonalization, the masses are only slightly changed and given by

$$\begin{aligned}\tilde{m} &= 773\dots 774 \text{ MeV} \\ \tilde{M}_V &= 2950\dots 2921 \text{ MeV},\end{aligned}\quad (3.16)$$

which would make the  $\omega$  meson 2–3 MeV lighter than the  $\rho$ , while in reality it is roughly 12 MeV heavier.

Larger effects could however arise for vector mesons that are comparable in mass with the vector glueball, such as charmonia, but for those the WSS model does not provide a reasonable description, because their masses are dominated by the quark masses whereas the vector mesons in the WSS model are independent of quark masses. Nevertheless, we can study the additional decay modes of vector charmonia that would be contributed by a certain mixing with vector glueballs. We shall return to this question after having determined the decay modes and partial widths of vector glueballs.

### C. Decays of the vector glueball

Except for the mixing term (3.10), all leading-order couplings of the vector glueball with ordinary mesons originating from the DBI action vanish, since they involve a

trace of commutator terms. Hence to this order all couplings arise through the Chern-Simons term and are thus anomalous. Further we note that  $C_3$  is dual to  $C_5$  since  $F_6 = \star F_4$ , leading to contributions from  $B_2$  as well as  $C_3$ .

From the Chern-Simons term of the D8-brane we obtain couplings to mesons, and through VMD also to photons, namely from

$$\begin{aligned}S_{\text{CS}}^{D8} &= T_8 \sum_p \int_{D8} \sqrt{\hat{A}(\mathcal{R})} \text{Tr} \exp(2\pi\alpha' F + B) \wedge C_p \\ &\supset T_8 \int_{D8} \text{Tr} \frac{(2\pi\alpha')^2}{2!} F \wedge F \wedge C_5 \\ &\quad + \text{Tr} \frac{(2\pi\alpha')^2}{2!} F \wedge F \wedge B_2 \wedge C_3.\end{aligned}\quad (3.17)$$

Looking at each term separately we have

$$F \wedge F \wedge C_5 = A \wedge F \wedge dC_5 = A \wedge F \wedge \star dC_3 \quad (3.18)$$

$$F \wedge F \wedge B_2 \wedge C_3 = A \wedge F \wedge B_2 \wedge F_4. \quad (3.19)$$

In the first term we can use the Hodge dual to fill the indices pertaining to the  $S_4$ . In the second term we can distribute the indices to obtain the  $F_4$  field strength from the background and  $B_{\mu z}$ . Note that for the field strengths with  $p > 4$  we have the twisted field strengths [54]

$$\begin{aligned}F_{p+1} &= dC_p - H \wedge C_{p-2} \\ &= (-1)^{p(p-1)/2} \star F_{9-p}, \quad p > 4\end{aligned}\quad (3.20)$$

but they are not dynamical [55].

From (3.18) we obtain

$$\begin{aligned}A \wedge F \wedge \star dC_3 &= -\frac{1}{2} \frac{1}{6g_s} \sqrt{-g} g^{\tau\tau} ((g^{\mu\sigma} g^{\nu\kappa} g^{\lambda\rho} + 2g^{\mu\kappa} g^{\nu\lambda} g^{\rho\sigma}) A_\mu F_{\nu\rho} \partial_\sigma C_{\kappa\lambda\tau} \\ &\quad + g^{zz} g^{\mu\rho} g^{\nu\sigma} (A_z F_{\mu\nu} + 2A_\mu F_{\nu z}) \partial_z C_{\rho\sigma\tau}) d^4 x dz d\Omega_4 \\ &= -\frac{1}{2} \frac{1}{6g_s} \sqrt{-g} g^{\tau\tau} \left( a(z) g^{\mu\kappa} g^{\nu\lambda} g^{\rho\delta} A_\mu F_{\nu\rho} \frac{1}{\sqrt{\square}} (\partial_\kappa \star F_{\lambda\delta}^V + \partial_\delta \star F_{\kappa\lambda}^V + \partial_\lambda \star F_{\delta\kappa}^V) \right. \\ &\quad \left. + g^{zz} g^{\mu\kappa} g^{\nu\lambda} (2A_z \partial_\mu A_\nu + 2A_\mu \partial_\nu A_z - 2A_\mu \partial_z A_\nu - 3iA_z [A_\mu, A_\nu]) \partial_z \frac{a(z)}{\sqrt{\square}} \star F_{\kappa\lambda}^V \right) d^4 x dz d\Omega_4 \\ &= -\frac{1}{6g_s} \sqrt{-g} g^{\tau\tau} \left( -\frac{a(z)}{2} g^{\mu\kappa} g^{\nu\lambda} g^{\rho\delta} A_\mu F_{\nu\rho} \epsilon_{\kappa\lambda\delta\sigma} \sqrt{\square} \eta^{\sigma\alpha} V_\alpha \right. \\ &\quad \left. + g^{zz} g^{\mu\kappa} g^{\nu\lambda} (A_z \partial_\mu A_\nu + A_\mu \partial_\nu A_z - A_\mu \partial_z A_\nu - \frac{3i}{2} A_z [A_\mu, A_\nu]) \partial_z \frac{a(z)}{\sqrt{\square}} \star F_{\kappa\lambda}^V \right) d^4 x dz d\Omega_4,\end{aligned}\quad (3.21)$$

and from (3.19)

$$\begin{aligned}
& A \wedge F \wedge B_2 \wedge F_4 \\
&= \frac{1}{2 \cdot 2} \epsilon^{MNO PQ} A_M F_{NO} B_{PQ} \left( \frac{3R^3}{g_s} \right) d^4 x dz d\Omega_4 \\
&= \frac{1}{2} \epsilon^{\mu\nu\rho\sigma} A_\mu F_{\nu\rho} B_{\sigma z} \left( \frac{3R^3}{g_s} \right) d^4 x dz d\Omega_4 \\
&= \frac{a(z)}{z} \epsilon^{\mu\nu\rho\sigma} A_\mu F_{\nu\rho} \frac{1}{\sqrt{\square}} V_\sigma \left( \frac{3R^3}{g_s} \right) d^4 x dz d\Omega_4, \quad (3.22)
\end{aligned}$$

where  $\star F_{\mu\nu}^V = \sqrt{\square} \tilde{C}_{\mu\nu}$ . Furthermore we utilized the full antisymmetry to rewrite

$$\begin{aligned}
(\partial_\mu \star F_{\nu\rho}^V + \partial_\nu \star F_{\rho\mu}^V + \partial_\rho \star F_{\mu\nu}^V) &= -\frac{1}{2} \epsilon_{\mu\nu\rho\sigma} \epsilon^{\sigma\alpha\beta\gamma} \partial_\alpha \star F_{\beta\gamma}^V \\
&= -\frac{1}{4} \epsilon_{\mu\nu\rho\sigma} \epsilon^{\sigma\alpha\beta\gamma} \partial_\alpha \epsilon_{\beta\gamma\lambda\kappa} F_V^{\lambda\kappa} \\
&= -\epsilon_{\mu\nu\rho\sigma} \partial_\alpha F_V^{\alpha\sigma} \\
&= -\epsilon_{\mu\nu\rho\sigma} \square V^\sigma. \quad (3.23)
\end{aligned}$$

Interactions between the vector glueball, pseudoscalar mesons, and vector mesons are thus given by

$$\mathcal{L}_{G_V \Pi v} = -\frac{1}{M_V} g_1^m \text{tr}(\Pi \partial_\mu v_\nu^{(m)} + v_\mu^{(m)} \partial_\nu \Pi) \star F_{\mu\nu}^V \quad (3.24)$$

where

$$\begin{aligned}
g_1^m &= \frac{9}{16} \sqrt{\frac{\kappa}{\pi}} \frac{1}{M_{\text{KK}}^2 R^3} \int dz \frac{1}{z} \psi_{2m-1}(z) \partial_z(z M_4(z)) \\
&= \frac{\{15.04, \dots\}}{\sqrt{\lambda} N_c}, \quad (3.25)
\end{aligned}$$

and we explicitly pulled out the mass dependence in the Lagrangian and used  $A_z = \Pi(x^\mu) K^{-1} / \sqrt{\kappa \pi M_{\text{KK}}^2}$ . The couplings to vector- and axial vector mesons are governed by

$$\begin{aligned}
\mathcal{L}_{G_V \rightarrow va} &= \frac{1}{M_V} f_1^{mn} \epsilon^{\mu\nu\rho\sigma} \text{tr}(v_\mu^m \partial_\nu a_\rho^n + a_\mu^n \partial_\nu v_\rho^m) V_\sigma \\
&\quad + \frac{1}{M_V} f_2^{mn} \text{tr}(v_\mu^m a_\nu^n) \star F_{\mu\nu}, \quad (3.26)
\end{aligned}$$

where

$$\begin{aligned}
f_1^{mn} &= \frac{3}{8} \frac{\kappa}{M_{\text{KK}} R^3} \int dz \left( \frac{3}{2} (1+z^2)^{-1/3} \frac{M_V^2}{M_{\text{KK}}^2} + 36 \right) \\
&\quad \times \psi_{2m-1}(z) \psi_{2n}(z) M_4(z) \\
&= \frac{\{177.83, \dots\} M_{\text{KK}}}{N_c \sqrt{\lambda}} \\
f_2^{mn} &= \frac{3}{8} \frac{\kappa}{M_{\text{KK}} R^3} \int dz \left( \frac{3}{2} \frac{1+z^2}{z} \right) (\psi_{2m-1} \psi'_{2n} - \psi'_{2m-1} \psi_{2n}) \\
&\quad \times \partial_z(z M_4(z)) \\
&= \frac{\{16.60, \dots\} M_{\text{KK}}}{N_c \sqrt{\lambda}}. \quad (3.27)
\end{aligned}$$

Note that since  $M_V \propto M_{\text{KK}}$ , (3.26) does not depend explicitly on the compactification scale.

The leading quartic couplings are obtained from the commutator terms in the non-Abelian field strengths  $F_{MN} = \partial_M A_N - \partial_N A_M - i[A_M, A_N]$  of the Chern-Simons interactions. To leading order we have

$$\mathcal{L}_{G_V \rightarrow \Pi v v} = \frac{i}{M_V} g_1^{mn} \text{tr}(\Pi [v_\mu^{(m)}, v_\nu^{(n)}]) \star F_{\mu\nu}^V \quad (3.28)$$

with

$$\begin{aligned}
g_1^{mn} &= \frac{9}{16} \sqrt{\frac{\kappa}{\pi}} \frac{1}{M_{\text{KK}}^2 R^3} \int dz \frac{1}{z} \psi_{2m-1}(z) \psi_{2n-1}(z) \partial_z(z M_4(z)) \\
&= \frac{\{1061, \dots\}}{\lambda N_c^{3/2}}. \quad (3.29)
\end{aligned}$$

Finally, there are interactions with one axial vector meson and two vector mesons. With the masses obtained by the WSS model, these are however at the mass threshold of the vector glueball, and even above the mass threshold of the pseudovector glueball, which is why they will not be considered in the following.

### 1. Hadronic decays

From Eq. (3.24) we obtain the squared amplitude for the decay into one pseudoscalar and one vector meson

$$\begin{aligned}
|\mathcal{M}_{G_V \rightarrow \Pi v^m}|^2 &= 2(g_1^m M_V \text{tr} T_\Pi T_v)^2 \\
&\quad \times \left( 1 - 2 \frac{m_\Pi^2 + m_v^2}{M_V^2} + \left( \frac{m_\Pi^2 - m_v^2}{M_V^2} \right)^2 \right) \quad (3.30)
\end{aligned}$$

with decay rate

$$\Gamma_{G_V \rightarrow \Pi v^m} = \frac{1}{3} \frac{|\mathbf{p}_v|}{8\pi M_V^2} |\mathcal{M}_{G_V \rightarrow \Pi v^m}|^2. \quad (3.31)$$

The resulting decay rates are collected in Table I.

From Eq. (3.26) we obtain the squared amplitude for the decay into one axial-vector and one vector meson as

$$\begin{aligned}
|\mathcal{M}_{G_V \rightarrow a^n v^n}|^2 = & \left( \frac{\text{tr} T_a T_v}{m_a m_v M_V} \right)^2 \left( f_1^{mn} f_2^{mn} (m_a^2 - m_v^2) (-2M_V^2 (m_a^2 + m_v^2) + 10m_a^2 m_v^2 + m_a^4 + m_v^4 + M_V^4) \right. \\
& + \frac{(f_1^{mn})^2}{2M_V^2} (M_V^6 (m_a^2 + m_v^2) - 2M_V^4 (6m_a^2 m_v^2 + m_a^4 + m_v^4) \\
& + M_V^2 (m_a^2 + m_v^2) (14m_a^2 m_v^2 + m_a^4 + m_v^4) + 4m_a^2 m_v^2 (m_a^2 - m_v^2)^2) \\
& \left. + \frac{(f_2^{mn})^2}{2} (M_V^4 (m_a^2 + m_v^2) - 2M_V^2 (-4m_a^2 m_v^2 + m_a^4 + m_v^4) + (m_a^2 - m_v^2)^2 (m_a^2 + m_v^2)) \right). \quad (3.32)
\end{aligned}$$

For the three-body decays (3.28) yields

$$\begin{aligned}
|\mathcal{M}_{G_V \rightarrow \Pi v^m v^n}|^2 = & \frac{(g_1^{mn})^2}{m_{v_1}^2 m_{v_2}^2 M_V^2} \left( m_{\Pi}^2 (m_{v_1}^2 (m_{v_2}^2 + M_V^2 - s_{12}) + M_V^2 (m_{v_2}^2 - M_V^2 + s_{12}) + s_{23} (M_V^2 - m_{v_2}^2 + s_{12})) \right. \\
& + m_{v_2}^2 M_V^2 (2M_V^2 - s_{12}) + s_{23} (m_{v_2}^2 (s_{12} - 4M_V^2) + s_{12} (M_V^2 - s_{12})) \\
& + m_{v_1}^2 (m_{v_2}^2 (17M_V^2 - 3(s_{12} + s_{23})) + m_{v_2}^4 + (M_V^2 - s_{12}) (2M_V^2 - 2s_{12} - s_{23})) \\
& \left. + m_{\Pi}^4 (-M_V^2) + s_{23}^2 (2m_{v_2}^2 - s_{12}) + m_{v_1}^4 m_{v_2}^2 \right) (\text{tr} T_{\Pi} [T_{v_1}, T_{v_2}])^2, \quad (3.33)
\end{aligned}$$

where  $s_{ij}$  is the center of mass energy of the vector meson and pseudoscalar subsystem.

Because  $a_1$  decays into  $\rho\pi$  with a large decay width, which as mentioned above is in fact rather well reproduced by the WSS model, we should consider the decay channels

TABLE I. Hadronic decays of the vector glueball with WSS model mass  $M_V = 2882$  MeV (mixing between vector glueball and singlet vector mesons neglected). Because of the large width of  $a_1 \rightarrow \rho\pi$ , the strongly interfering direct and resonant decays into  $\rho\rho\pi$  have been combined.

	$\Gamma_{G_V(2882)}$ [MeV]
$G_V \rightarrow \rho\pi$	34.3...45.4
$G_V \rightarrow K^*K$	37.8...50.1
$G_V \rightarrow \omega\eta$	5.78...9.80
$G_V \rightarrow \phi\eta$	3.45...2.81
$G_V \rightarrow \omega\eta'$	3.06...2.50
$G_V \rightarrow \phi\eta'$	3.22...5.46
$G_V \rightarrow a_1\rho, \rho\rho\pi$	339...417
$G_V \rightarrow K_1(1270)K^*$	185...246
$G_V \rightarrow K_1(1400)K^*$	320...424
$G_V \rightarrow f_1\omega$	212...281
$G_V \rightarrow f_1'\omega$	22.4...29.7
$G_V \rightarrow f_1\phi$	9.51...12.6
$G_V \rightarrow f_1'\phi$	47.8...63.3
$G_V \rightarrow K^*K^*\pi$	22.7...39.9
$G_V \rightarrow K^*\rho K$	30.3...53.2
$G_V \rightarrow K^*\omega K$	9.85...17.3
$G_V \rightarrow K^*K^*\eta$	7.77...12.1
$G_V \rightarrow \phi K^*K$	3.87...6.80
$G_V \rightarrow \text{hadrons}$	1301...1725

$a_1\rho$  and  $\rho\rho\pi$  together (see Fig. 1), since these decays can interfere either positively or negatively. In fact, we find that there is almost maximal negative interference. In isolation,  $G_V \rightarrow a_1\rho$  would have a partial width of 822...1089 MeV, whereas the resonant decay  $G_V \rightarrow a_1\rho \rightarrow \rho\rho\pi$  together with the nonresonant  $G_V \rightarrow \rho\rho\pi$  is only about 60% of that.

When extending these results to the axial vector mesons involving strange quarks, we instead treat those as narrow

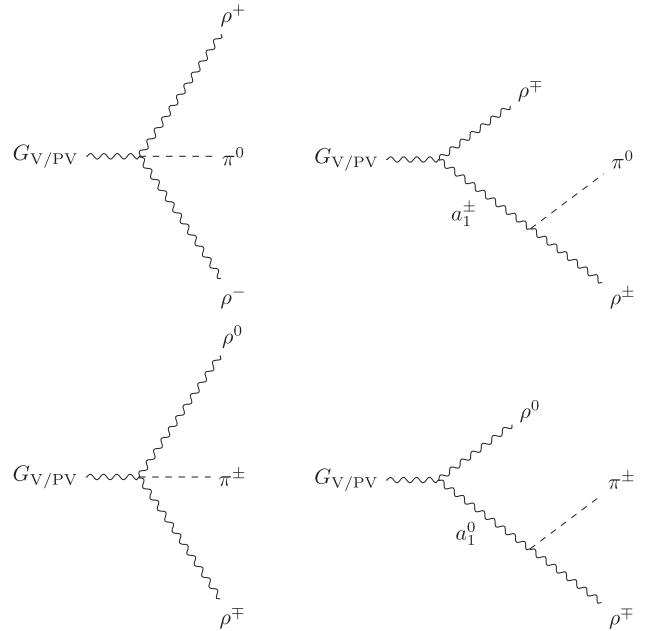


FIG. 1. Feynman diagrams contributing to the hadronic three body decay of the vector glueball into  $\rho\rho\pi$ .



resonances and final decay products, neglecting the corresponding interference effects. In fact, in real QCD the axial vector mesons  $K_1$  and  $f_1$  have much smaller decay widths. Using their experimental widths indeed leads to comparatively minor changes of the combined resonant plus nonresonant three-body decays.

## 2. Comparison with Ref. [56]

In Ref. [56], Giacosa *et al.* have calculated branching ratios for the vector glueball resulting from three candidate interaction terms in a chiral Lagrangian inspired by the extended linear sigma model (eLSM) developed in [14,57–59]. Since there is no experimental information on the coupling constants in either of those terms, ratios of partial decay widths within each of the three possibilities have been worked out. Two of these terms involve dimension-4 operators and do not have a counterpart in the WSS model studied here, so the latter suggests that they may be subleading. A third one breaks dilatation invariance and involves the Levi-Civita tensor that appears also in all the interactions following from the Chern-Simons term in the WSS model, but the resulting interactions differ qualitatively from those considered in Ref. [56]. In particular, there are terms in (3.26) which cannot be written in terms of the (dual) field strength tensor for the vector glueball field, whereas Ref. [56] considered only one term proportional to  $\star F^V$ .

In Table II, our results for the ratios of the various partial decay widths and  $\Gamma(G_V \rightarrow \rho\pi)$  are compared with Ref. [56]. In both models the dominant decay mode is  $G_V \rightarrow a_1\rho$ , but in the WSS model this is a factor of 24 larger than  $\Gamma(G_V \rightarrow \rho\pi)$ , while in the model of Ref. [56] this factor is 1.8, more than an order of magnitude smaller.<sup>4</sup> The second strongest decay mode is  $K_1K^*$ , for which Ref. [56] does not list a result, followed by  $f_1\omega$ . The WSS model thus predicts a rather strong enhancement of decays into a pair of axial vector and vector compared to a pair of pseudoscalar and vector.

## 3. Radiative decays

From Eq. (3.24) we obtain the coupling to photons by utilizing VMD

$$\mathcal{L}_{G_V\Pi\gamma} = \frac{1}{M_V} g_1^\gamma \text{tr}(\Pi\partial_\mu\mathcal{V}_\nu + \mathcal{V}_\mu\partial_\nu\Pi)\star F_{\mu\nu}^V \quad (3.34)$$

where

$$g_1^\gamma = \frac{9}{16} \sqrt{\frac{\kappa}{\pi}} \frac{1}{M_{\text{KK}}^2 R^3} \int dz \frac{1}{z} \partial_z(zM_4(z)) = \frac{0.31}{\sqrt{N_c}}. \quad (3.35)$$

<sup>4</sup>Here we are taking into account the substantial negative interference with nonresonant  $G_V \rightarrow \rho\rho\pi$  decays in the WSS model, while [56] considered only two-body decays.

TABLE II. Relative branching ratios of the hadronic decays of the vector glueball with WSS model mass  $M_V = 2882$  MeV and with quenched lattice QCD result [7] 3830 MeV, the latter for the sake of comparison with Ref. [56].

	$\frac{\Gamma_{G_V(2882) \rightarrow \dots}}{\Gamma_{G_V(2882) \rightarrow \rho\pi}}$	$\frac{\Gamma_{G_V(3830) \rightarrow \dots}}{\Gamma_{G_V(3830) \rightarrow \rho\pi}}$	Reference [56]
$\rho\pi$	1	1	1
$K^*K$	1.1	1.21	1.3
$\omega\eta$	0.17...0.22	0.18...0.23	0.16
$\phi\eta$	0.10... 0.062	0.12...0.07	0.21
$\omega\eta'$	0.089... 0.055	0.11...0.07	0.13
$\phi\eta'$	0.094... 0.12	0.14...0.18	0.18
$a_1\rho, \rho\rho\pi$	9.88...9.18	17.0...15.3	1.8
$K_1(1270)K^*$	5.40	12.0	
$K_1(1400)K^*$	9.32	23.8	
$f_1\omega$	6.2	11.8	0.55
$f_1'\omega$	0.65	1.41	0.82
$f_1\phi$	0.28	0.83	
$f_1'\phi$	1.4	4.92	
$K^*K^*\pi$	0.66...0.88	1.92...2.54	
$K^*\rho K$	0.88...1.17	3.48...4.62	
$K^*\omega K$	0.29...0.38	1.14...4.62	
$K^*K^*\eta$	0.23...0.27	1.19...1.40	
$\phi K^*K$	0.11...0.15	0.70...0.93	

Employing VMD in Eq. (3.26) we readily obtain the coupling between the vector glueball, an axial vector meson, and one photon as

$$\begin{aligned} \mathcal{L}_{\text{CS}}^{\text{D}8} \supset & \frac{1}{M_V} f_1^{\gamma n} \epsilon^{\mu\nu\rho\sigma} \text{tr}(\mathcal{V}_\mu \partial_\nu a_\rho^n + a_\mu^n \partial_\nu \mathcal{V}_\rho) V_\sigma \\ & + \frac{1}{M_V} f_2^{\gamma n} \epsilon^{\mu\nu\rho\sigma} \text{tr}(\mathcal{V}_\mu \partial_\nu a_\rho^n - a_\mu^n \partial_\nu \mathcal{V}_\rho) V_\sigma, \end{aligned} \quad (3.36)$$

where

$$\begin{aligned} f_1^{\gamma n} &= \frac{3}{8} \frac{\kappa}{M_{\text{KK}} R^3} \int dz \left( \frac{3}{2} (1+z^2)^{-1/3} \frac{M_V^2}{M_{\text{KK}}^2} + 36 \right) \\ & \quad \times \psi_{2n}(z) M_4(z) = \frac{\{5.88, \dots\} M_{\text{KK}}}{\sqrt{N_c}} \\ f_2^{\gamma n} &= \frac{3}{8} \frac{\kappa}{M_{\text{KK}} R^3} \int dz \left( \frac{3}{2} \frac{1+z^2}{z} \right) \psi'_{2n}(z) \partial_z(zM_4(z)) \\ &= \frac{\{0.36, \dots\} M_{\text{KK}}}{\sqrt{N_c}}, \end{aligned} \quad (3.37)$$

and the Lagrangian is again independent of the compactification scale. The quartic coupling including one photon is obtained in a similar fashion from Eq. (3.28)

$$\mathcal{L}_{G_V \rightarrow \Pi\gamma} = \frac{i}{M_V} g_1^{m\gamma} 2 \text{tr}(\Pi[\mathcal{V}_\mu, v_\nu^{(m)}]) \star F_{\mu\nu}^V, \quad (3.38)$$

where

$$\begin{aligned}
 g_1^{m\nu} &= \frac{27}{32} \sqrt{\frac{\bar{\kappa}}{\pi}} \frac{1}{M_{\text{KK}}^2 R^3} \int dz \frac{1}{z} \psi_{2m-1}(z) \partial_z (z M_4(z)) \\
 &= \frac{\{22.55, \dots\}}{\sqrt{\lambda} N_c}.
 \end{aligned} \quad (3.39)$$

From Eq. (3.24) the squared amplitude for the decay into one pseudoscalar and one photon is obtained as

$$|\mathcal{M}_{G_V \rightarrow \Pi \nu}|^2 = 2(e g_1^{\nu} \text{tr} T_{\Pi} Q)^2 M_V^2 \left(1 - \frac{m_{\Pi}^2}{M_V^2}\right)^2 \quad (3.40)$$

with decay rate

$$\begin{aligned}
 |\mathcal{M}_{G_V \rightarrow \Pi \nu}|^2 &= \frac{2(g_1^{m\nu})^2}{m_v^2 M_V^2 (M_V^2 - s_{12})^2} \left(2m_v^2 M_V^2 \left[(s_{12} - M_V^2)(m_{\Pi}^2 - 3M_V^2 + 2s_{12}) - s_{23}(M_V^2 + s_{12})\right] \right. \\
 &\quad \left. + (m_{\Pi}^2 - s_{12})^2 (M_V^2 - s_{12})^2 + 2s_{12}s_{23}(m_{\Pi}^2 - s_{12})(M_V^2 - s_{12}) + 2m_v^4 M_V^4 + s_{23}^2 (M_V^4 + s_{12}^2)\right).
 \end{aligned} \quad (3.43)$$

There are no three-body decays with two external photons due to the appearance of the commutator in Eq. (3.38). But there are also decays into one photon, one vector meson, and one axial vector meson determined by

$$\mathcal{L}_{G_V \rightarrow a \nu} = -\frac{3i}{M_V} f_1^{mn} \epsilon^{\mu\nu\rho\sigma} \text{tr} \mathcal{V}_{\mu} [v_{\nu}^m, a_{\rho}^n] V_{\sigma}, \quad (3.44)$$

with the same coupling  $f_1^{mn}$  as in (3.27) that dominated the hadronic decays.

The various partial decay widths are collected in Table III. Again we combine  $\rho\pi$  decay products with resonant  $a_1 \rightarrow \rho\pi$  contributions (see Fig. 2) although here the interference is of lesser importance.

#### 4. Implications for the $\rho\pi$ puzzle

A long-standing puzzle in charmonium physics is the experimental fact that the radial excitation  $\psi' = \psi(2S) = \psi(3686)$  of the vector meson  $J/\psi$  has decays into  $\rho\pi$ ,  $K^*K$ ,

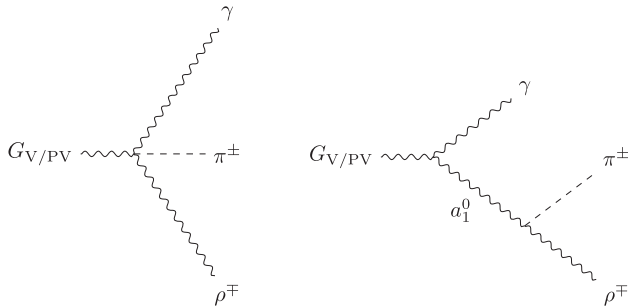


FIG. 2. Feynman diagrams contributing to the radiative three body decay of the vector glueball into  $\pi\rho\gamma$ .

$$\Gamma_{G_V \rightarrow \Pi \nu} = \frac{1}{3} \frac{|\mathbf{p}_\nu|}{8\pi M_V^2} |\mathcal{M}_{G_V \rightarrow \Pi \nu}|^2. \quad (3.41)$$

From Eq. (3.36) we obtain the squared amplitude for the decay into one axial vector meson and one photon

$$\begin{aligned}
 |\mathcal{M}_{G_V \rightarrow a \nu}|^2 &= \frac{\text{tr} T_a Q^2}{2m_a^2 M_V^4} (-2M_V^2 f_1^{n\nu} f_2^{n\nu} (-2m_a^2 M_V^2 - 7m_a^4 + M_V^4) \\
 &\quad + (f_1^{n\nu})^2 (9m_a^4 M_V^2 - 6m_a^2 M_V^4 + 4m_a^6 + M_V^6) \\
 &\quad + M_V^2 (f_2^{n\nu})^2 (6m_a^2 M_V^2 + m_a^4 + M_V^4)).
 \end{aligned} \quad (3.42)$$

The squared amplitude for the three-body decays resulting from Eq. (3.38) is given by

and other hadronic channels with partial widths far below the expectation from their nature of a nonrelativistic bound state of  $c$  and  $\bar{c}$  [34,60].

Early attempts to explain this are based on a mixing of the ground state  $J/\psi$  with a vector glueball that enhances the decay modes involved in the  $\rho\pi$  puzzle [31–33,61–63], for instance by assuming a narrow vector glueball with mass close to that of  $J/\psi$  so that a resonant enhancement of the mixing appears [cf. (3.13)].

The WSS model is certainly not suitable to describe the nonrelativistic  $c\bar{c}$  bound states, but it makes concrete predictions for the decays of the vector glueball. Since the vector glueball is predicted to be a rather wide resonance, it does not fit the picture assumed in [32].

TABLE III. Radiative decays of the vector glueball with WSS model mass  $M_V = 2882$  MeV.

	$\Gamma_{G_V(2882)}$ [keV]
$G_V \rightarrow \pi^0 \gamma$	27.8
$G_V \rightarrow \eta \gamma$	7.85... 6.96
$G_V \rightarrow \eta' \gamma$	0.40...1.10
$G_V \rightarrow a_1 \gamma, \rho \pi \gamma$	358...361
$G_V \rightarrow f_1 \gamma$	41.5
$G_V \rightarrow f_1' \gamma$	11.4
$G_V \rightarrow K^* K \gamma$	78.2...104
$G_V \rightarrow a_1 \rho \gamma$	338...447
$G_V \rightarrow K_1(1270) K^* \gamma$	47.2...62.6
$G_V \rightarrow K_1(1400) K^* \gamma$	47.3...62.7
$G_V \rightarrow X + \gamma$	958...1126

Moreover, lattice QCD predicts a mass of the vector glueball about 700 MeV higher than that of  $J/\psi$ . Nevertheless, it is not excluded that the mixing of the vector glueball could be strongly different for the different vector charmonia. Indeed, in Sec. III B 2, we have found that the mixing of excited vector mesons depends strongly on the mode number, albeit the first two modes happened to be comparable, but that need not be the case for vector mesons far from the chiral limit.

However, the decay pattern that we have obtained for the vector glueball makes it rather unsuitable for an explanation of the  $\rho\pi$  puzzle. While the vector glueball has  $\rho\pi$  and  $K^*K$  as important decay modes, decays into  $a_1\rho$  and  $K_1(1400)K^*$  are much stronger, but have not been observed in the hadronic decays of  $J/\psi$  [64].

#### IV. REVISITING THE PSEUDOVECTOR GLUEBALL

After Kaluza-Klein reduction of the 3 form field  $A_3$  of the 11D supergravity theory to 10D, the  $1^{+-}$  glueball is identified with the fluctuations of  $B_{\mu\nu} = A_{\mu\nu 11}$  and  $C_{\mu\tau r} = A_{\mu\tau r}$ . In 10D notation the equations of motion are solved by

$$\begin{aligned} B_{\mu\nu} &= c(u)\tilde{B}_{\mu\nu}(x^\mu), \\ C_{\mu\tau u} &= \frac{3}{2g_s\Box} \frac{c(u)}{u} \eta_{\mu\nu} \epsilon^{\nu\rho\sigma\kappa} \partial_\rho \tilde{B}_{\sigma\kappa}(x^\mu). \end{aligned} \quad (4.1)$$

Upon rescaling  $c(u) = (r/r_{\text{KK}})^3 N_4(r)$ ,  $u^3 = r^6/r_{\text{KK}}^6$ , the radial mode corresponds to the one already obtained in [30]. In terms of the  $z$  coordinate this rescaling amounts to  $c(z) = \sqrt{1+z^2} N_4(z)$ , hence the  $N_4$  mode has even  $z$  parity.

In [23] only the Chern-Simons couplings arising from  $B_2$  were considered. However, there is an additional coupling arising from the dualization of  $F_6 = \star F_4$  which has been overlooked. Inducing the pseudovector fluctuation on this term we obtain additionally

$$\begin{aligned} A \wedge F \wedge \star dC_3 &= \frac{1}{4!} \sqrt{-g} A_M F_{NO} F_4^{\tau MNO} d^4x dz d\Omega_4 \\ &= \frac{1}{3! M_{\text{PV}}} \sqrt{-g} g^{zz} g^{\tau\tau} (A_z F_{\mu\nu} + 2A_\mu F_{\nu z}) \\ &\quad \times F_{\tilde{\nu}}^{\mu\nu} \frac{3}{2g_s} z^2 c(z) d^4x dz d\Omega_4, \end{aligned} \quad (4.2)$$

besides the couplings already computed in [23]

$$\begin{aligned} A \wedge F \wedge B_2 \wedge F_4 &= -\frac{c(z)}{2M_{\text{PV}}} (A_z F_{\mu\nu} + 2A_\mu F_{\nu z}) \\ &\quad \times F_{\mu\nu}^{\tilde{\nu}} \left( \frac{3R^3}{g_s} \right) d^4x dz d\Omega_4. \end{aligned} \quad (4.3)$$

From this we obtain

$$\mathcal{L}_{G_{\text{PV}} \rightarrow \Pi\nu} = -\left(1 - \frac{1}{3!}\right) \frac{1}{M_{\text{PV}}} b_1^m \text{tr}(v_\mu^{(m)} \partial_\nu \Pi + \Pi \partial_\mu v_\nu^{(m)}) F_{\mu\nu}^{\tilde{\nu}} \quad (4.4)$$

where the first term is the one already obtained in [23], and the second term involving  $-\frac{1}{3!}$  arises through the dualization of  $C_3$ , with

$$\begin{aligned} b_1^m &= T_8 \frac{(2\pi\alpha')^2 3R^3}{2! g_s} \left( \frac{8\pi^2}{3} \right) \int dz K^{-1/2} \psi_{2m-1}(z) N_4(z) \\ &= \frac{27}{4} \sqrt{\frac{\kappa}{\pi M_{\text{KK}}^2 R^3}} \int \frac{dz}{\sqrt{1+z^2}} \psi_{2m-1}(z) N_4(z) \\ &= \frac{\{112.054, \dots\}}{\sqrt{\lambda} N_c}. \end{aligned} \quad (4.5)$$

This results in a reduction of the decay rates of roughly 30%.

The corresponding coupling to the photon is readily obtained as

$$\mathcal{L}_{G_{\text{PV}} \rightarrow \Pi\gamma} = -\frac{5}{6} \frac{1}{M_{\text{PV}}} b_1^\gamma \text{tr}(\mathcal{V}_\mu \partial_\nu \Pi + \Pi \partial_\mu \mathcal{V}_\nu) F_{\mu\nu}^{\tilde{\nu}}, \quad (4.6)$$

where

$$b_1^\gamma = \frac{27}{4} \sqrt{\frac{\kappa}{\pi M_{\text{KK}}^2 R^3}} \int \frac{dz}{\sqrt{1+z^2}} N_4(z) = \frac{2.70}{\sqrt{N_c}}. \quad (4.7)$$

There is also a coupling between the pseudovector glueball and vector- and axial vector mesons present, which has not been considered in [23]. Their masses are, however, at the threshold of the WSS model mass. Explicitly it is given by

$$\mathcal{L}_{G_{\text{PV}} \rightarrow \nu a} = -\frac{5}{6} \frac{1}{M_{\text{PV}}} b_3^{mn} \text{tr}(v_\mu^{(m)} a_\nu^{(n)}) F_{\mu\nu}^{\tilde{\nu}} \quad (4.8)$$

with

$$\begin{aligned} b_3^{mn} &= \frac{27}{4} \frac{\kappa}{M_{\text{KK}} R^3} \int dz \sqrt{1+z^2} (\psi_{2m-1}(z) \psi'_{2n}(z) \\ &\quad - \psi'_{2m-1}(z) \psi_{2n}(z)) N_4(z) \\ &= \frac{\{118.66, \dots\} M_{\text{KK}}}{\sqrt{\lambda} N_c}. \end{aligned} \quad (4.9)$$

This entails a coupling to photons and axial vector mesons given by

$$\mathcal{L}_{G_{\text{PV}} \rightarrow \gamma a} = -\frac{5}{6} \frac{1}{M_{\text{PV}}} b_3^{\nu\gamma} \text{tr}(\mathcal{V}_\mu a_\nu^{(m)}) F_{\mu\nu}^{\tilde{\nu}} \quad (4.10)$$

with

$$\begin{aligned} b_3^{\nu\gamma} &= \frac{27}{4} \frac{\kappa}{M_{\text{KK}} R^3} \int dz \sqrt{1+z^2} \psi_{2m-1}(z) \psi'_{2n}(z) N_4(z) \\ &= \frac{\{1.75, \dots\} M_{\text{KK}}}{\sqrt{N_c}}. \end{aligned} \quad (4.11)$$

Three-body decays result from the interactions governed by

TABLE IV. Hadronic decays of the pseudovector glueball with WSS model mass of  $M_{\text{PV}} = 2311$  MeV.

	$\Gamma_{G_{\text{PV}(2311)}} [\text{MeV}]$
$G_{\text{PV}} \rightarrow \rho\pi$	585...775
$G_{\text{PV}} \rightarrow K^*K$	259...338
$G_{\text{PV}} \rightarrow \eta\omega$	83.2...141
$G_{\text{PV}} \rightarrow \eta\phi$	13.8...11.3
$G_{\text{PV}} \rightarrow \eta'\omega$	31.9...26.0
$G_{\text{PV}} \rightarrow \eta'\phi$	5.21...8.83
$G_{\text{PV}} \rightarrow a_1\rho, \rho\rho\pi$	433...751
$G_{\text{PV}} \rightarrow K_1(1270)K^*$	26.9...35.6
$G_{\text{PV}} \rightarrow K_1(1400)K^*$	1.72...2.82
$G_{\text{PV}} \rightarrow f_1\omega$	40.9...54.2
$G_{\text{PV}} \rightarrow f_1'\omega$	1.32...1.75
$G_{\text{PV}} \rightarrow K^*K^*\pi$	37.6...66.0
$G_{\text{PV}} \rightarrow K^*\rho K$	5.85...10.3
$G_{\text{PV}} \rightarrow K^*\omega K$	1.66...2.91
$G_{\text{PV}} \rightarrow \text{hadrons}$	1476...2162

TABLE V. Hadronic decays of the pseudovector glueball with WSS model mass  $M_{\text{PV}} = 2311$  MeV and the quenched lattice value of 2980 MeV.

	$\frac{\Gamma_{G_{\text{PV}(2311)} \rightarrow \dots}}{\Gamma_{G_{\text{PV}(2311)} \rightarrow \rho\pi}}$	$\frac{\Gamma_{G_{\text{PV}(2980)} \rightarrow \dots}}{\Gamma_{G_{\text{PV}(2980)} \rightarrow \rho\pi}}$
$\rho\pi$	1	1
$K^*K$	0.55	0.75
$\omega\eta$	0.14...0.18	0.17...0.21
$\phi\eta$	0.02...0.01	0.04...0.03
$\omega\eta'$	0.05...0.03	0.09...0.06
$\phi\eta'$	0.009...0.01	0.04...0.05
$a_1\rho, \rho\rho\pi$	0.74...0.97	2.64...3.35
$K_1(1270)K^*$	0.05	0.16
$K_1(1400)K^*$	0.003	0.24
$f_1\omega$	0.07	0.16
$f_1'\omega$	0.002	0.015
$f_1\phi$		0.01
$f_1'\phi$		0.04
$K^*K^*\pi$	0.06...0.09	0.43...0.57
$K^*\rho K$	0.010...0.013	0.52...0.69
$K^*\omega K$	0.003...0.004	0.17...0.22
$K^*K^*\eta$		0.11...0.12
$\phi K^*K$		0.04...0.06

$$\mathcal{L}_{G_{\text{PV}}\Pi v v} = \frac{5}{6} \frac{i}{M_V} b_2^{mn} \text{tr}(\Pi[v_\mu^{(m)}, v_\nu^{(n)}]) F_{\mu\nu}^{\bar{V}} \quad (4.12)$$

where<sup>5</sup>

<sup>5</sup>Our results for  $b_1^m$  and  $b_2^{mn}$  for  $m = n = 1$  differ from the ones in [23] by factors of 2 and  $2^{3/2}$ , respectively, due to the different normalization of the  $SU(N_f)$  generators.

TABLE VI. Radiative decays of the pseudovector glueball with WSS model mass of  $M_{\text{PV}} = 2311$  MeV.

	$\Gamma_{G_{\text{PV}(2311)}} [\text{keV}]$
$G_{\text{PV}} \rightarrow \pi^0\gamma$	0.01
$G_{\text{PV}} \rightarrow \eta\gamma$	1.11...0.98
$G_{\text{PV}} \rightarrow \eta'\gamma$	0.59...1.62
$G_{\text{PV}} \rightarrow a_1\gamma, \rho\pi\gamma$	1395...1848
$G_{\text{PV}} \rightarrow f_1\gamma$	5.16
$G_{\text{PV}} \rightarrow f_1'\gamma$	1.40
$G_{\text{PV}} \rightarrow K^*K\gamma$	266...353
$G_{\text{PV}} \rightarrow X + \gamma$	1669...2209

$$b_2^{mn} = \frac{81}{8} \sqrt{\frac{\kappa}{\pi}} \frac{1}{M_{\text{KK}}^2 R^3} \int dz \psi_{2m-1}(z) \psi_{2n-1}(z) N_4(z) = \frac{\{7257.92, \dots\}}{\lambda N_c^{3/2}}, \quad (4.13)$$

with a corresponding photon coupling given by

$$\mathcal{L}_{G_{\text{PV}}\Pi v \nu} = \frac{5}{6} \frac{i}{M_V} 2b_2^{m\nu} \text{tr}(\Pi[v_\mu^{(m)}, \mathcal{V}_\nu]) F_{\mu\nu}^{\bar{V}} \quad (4.14)$$

with

$$b_2^{m\nu} = \frac{\{168.081, \dots\}}{\sqrt{\lambda} N_c}. \quad (4.15)$$

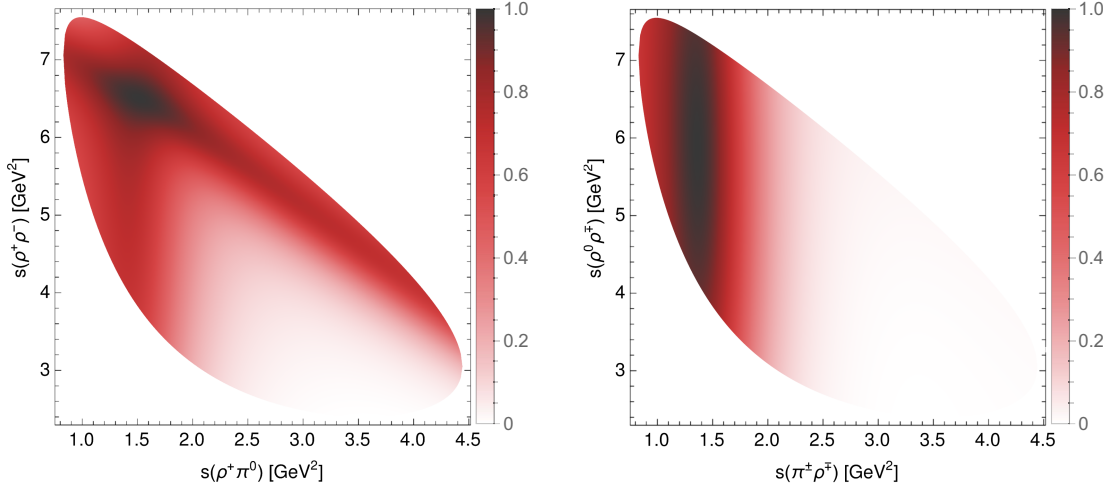
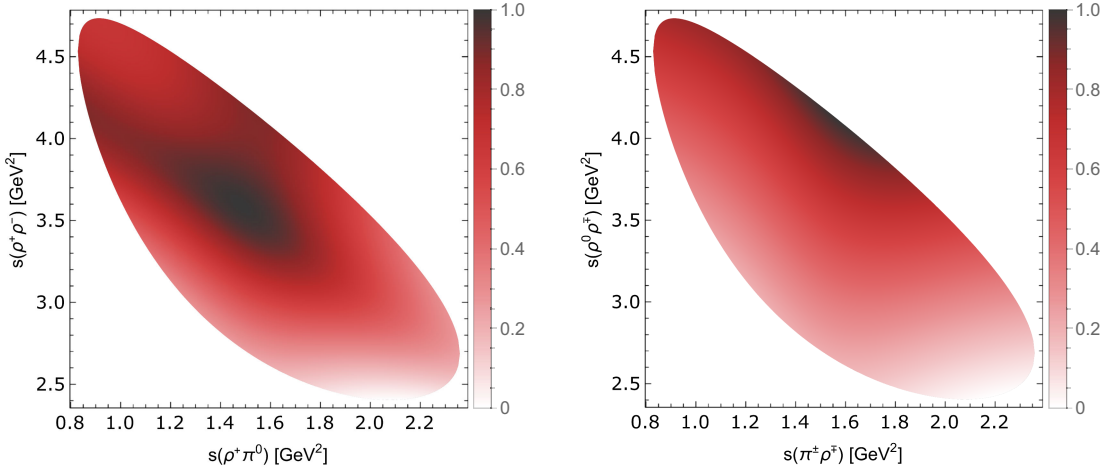
The results for the hadronic decay rates are collected in Table IV. Table V shows the change of the decay pattern when the WSS model mass  $M_{\text{PV}} = 2311$  MeV is replaced by the quenched lattice value of 2980 MeV. The radiative decays are displayed in Table VI; note that there is no analog of (3.44) and thus there are no  $av\gamma$  decays.

## V. CONCLUSION AND DISCUSSION

In this paper we have completed our previous study [25] of radiative and purely hadronic decays of glueballs in the WSS model by investigating the decay modes of spin-1 $^{\pm}$  glueballs. We have found that the latter are dominated by anomalous vertices involving the Levi-Civita symbol which are uniquely determined by the Chern-Simons action of the flavor branes.

In the case of the vector glueball, such anomalous decays have previously been studied by Giacosa *et al.* [56], however in the form of just one candidate term among others which are nonanomalous. While Ref. [56] also obtained  $a_1\rho$  decays as dominant anomalous decay, the branching ratio for vector-axial vector decay modes is very much higher in the WSS prediction. For pseudovector glueballs we instead found a dominance of  $\rho\pi$ .

The WSS model also has direct vertices for the spin-1 glueballs with two vector mesons together with one


 FIG. 3. Dalitz plots for the three body decay  $G_V \rightarrow \rho\rho\pi$ .

 FIG. 4. Dalitz plots for the three body decay  $G_{PV} \rightarrow \rho\rho\pi$ .

pseudoscalar. In the case of the  $a_1\rho$  channel we found that  $\rho\rho\pi$  interferes strongly and negatively with  $a_1\rho \rightarrow \rho\rho\pi$ . Whereas for vector glueballs  $a_1\rho$  has a much larger amplitude, for pseudovector glueballs it is below the direct  $\rho\rho\pi$  channel. In Figs. 3 and 4 we display the corresponding Dalitz plots for the two spin-1 glueballs with mass given by the WSS model, which shows that in the case of the vector glueball, the resonant decay via  $a_1$  should be visible. A clearer signal can however be expected for the decay channels  $G_V \rightarrow K_1(1400)K^*$  and  $G_V \rightarrow K_1(1270)K^*$  which arise in proportion to their  $K_{1A}$  content, since the strange axial vector mesons are more narrow resonances. When the vector glueball mass is extrapolated from the WSS model mass to the prediction of lattice QCD,  $K_1(1400)K^*$  becomes the leading mode.

The decay pattern of the vector glueball is thus conspicuously dominated by  $a_1\rho$  and  $K_1K^*$ , which could help in finding its signatures in reactions such as those studied in [65] but also implies that a mixing of  $J/\psi$  with the vector

glueball as proposed in [31–33,61–63] cannot explain the  $\rho\pi$  puzzle in  $J/\psi$  and  $\psi'$  decays.

We have also revisited the decay pattern of the pseudo-vector glueball of Ref. [23], confirming the conclusion of a very broad resonance, but correcting the result from  $\Gamma/M \sim 0.92\dots 1.37$  to  $0.64\dots 0.94$ . The heavier vector glueball has turned out to be only slightly less broad, with  $\Gamma/M \sim 0.45\dots 0.60$ . The large widths probably make both spin-1 glueballs difficult to detect. On the other hand, their interactions, which are strongly dominated<sup>6</sup> by anomalous vertices and which are numerically large, point to an important role in applications like those studied in Ref. [66].

<sup>6</sup>Nonanomalous pseudovector glueball interactions from quartic terms in the DBI action have been worked out in Ref. [23], where they were found to be negligibly small, suppressed by an extra inverse 't Hooft coupling as well as small coefficients.

## ACKNOWLEDGMENTS

We would like to thank Claude Amsler and Francesco Giacosa for useful discussions. F. H. and J. L. have been supported by the Austrian Science Fund (FWF), Project No. P 33655-N and the FWF doctoral program Particles & Interactions, Project No. W1252-N27.

- 
- [1] E. Klempt and A. Zaitsev, Glueballs, hybrids, multiquarks. Experimental facts versus QCD inspired concepts, *Phys. Rep.* **454**, 1 (2007).
- [2] V. Crede and C. A. Meyer, The experimental status of glueballs, *Prog. Part. Nucl. Phys.* **63**, 74 (2009).
- [3] W. Ochs, The status of glueballs, *J. Phys. G* **40**, 043001 (2013).
- [4] H.-X. Chen, W. Chen, X. Liu, Y.-R. Liu, and S.-L. Zhu, An updated review of the new hadron states, *Rep. Prog. Phys.* **86**, 026201 (2023).
- [5] G. S. Bali, K. Schilling, A. Hulsebos, A. C. Irving, C. Michael, and P. W. Stephenson (UKQCD Collaboration), A comprehensive lattice study of SU(3) glueballs, *Phys. Lett. B* **309**, 378 (1993).
- [6] C. J. Morningstar and M. J. Peardon, The glueball spectrum from an anisotropic lattice study, *Phys. Rev. D* **60**, 034509 (1999).
- [7] Y. Chen *et al.*, Glueball spectrum and matrix elements on anisotropic lattices, *Phys. Rev. D* **73**, 014516 (2006).
- [8] E. Gregory, A. Irving, B. Lucini, C. McNeile, A. Rago, C. Richards, and E. Rinaldi, Towards the glueball spectrum from unquenched lattice QCD, *J. High Energy Phys.* **10** (2012) 170.
- [9] F. Chen, X. Jiang, Y. Chen, K.-F. Liu, W. Sun, and Y.-B. Yang, Glueballs at physical pion mass, *Chin. Phys. C* **47**, 063108 (2023).
- [10] C. Amsler and F. E. Close, Is  $f_0(1500)$  a scalar glueball?, *Phys. Rev. D* **53**, 295 (1996).
- [11] F. E. Close and A. Kirk, Scalar glueball- $q\bar{q}$  mixing above 1 GeV and implications for lattice QCD, *Eur. Phys. J. C* **21**, 531 (2001).
- [12] F. E. Close and Q. Zhao, Production of  $f_0(1710)$ ,  $f_0(1500)$ , and  $f_0(1370)$  in  $J/\psi$  hadronic decays, *Phys. Rev. D* **71**, 094022 (2005).
- [13] W.-J. Lee and D. Weingarten, Scalar quarkonium masses and mixing with the lightest scalar glueball, *Phys. Rev. D* **61**, 014015 (2000).
- [14] S. Janowski, F. Giacosa, and D. H. Rischke, Is  $f_0(1710)$  a glueball?, *Phys. Rev. D* **90**, 114005 (2014).
- [15] H.-Y. Cheng, C.-K. Chua, and K.-F. Liu, Revisiting scalar glueballs, *Phys. Rev. D* **92**, 094006 (2015).
- [16] J.-M. Frère and J. Heeck, Scalar glueballs: Constraints from the decays into  $\eta$  or  $\eta'$ , *Phys. Rev. D* **92**, 114035 (2015).
- [17] E. Klempt, Scalar mesons and the fragmented glueball, *Phys. Lett. B* **820**, 136512 (2021).
- [18] S. Donnachie, H. G. Dosch, O. Nachtmann, and P. Landshoff, *Pomeron Physics and QCD* (Cambridge University Press, Cambridge, England, 2004), Vol. 19, p. 12.
- [19] K. Hashimoto, C.-I. Tan, and S. Terashima, Glueball decay in holographic QCD, *Phys. Rev. D* **77**, 086001 (2008).
- [20] F. Brünner, D. Parganlija, and A. Rebhan, Glueball decay rates in the Witten-Sakai-Sugimoto model, *Phys. Rev. D* **91**, 106002 (2015).
- [21] F. Brünner and A. Rebhan, Nonchiral enhancement of scalar glueball decay in the Witten-Sakai-Sugimoto model, *Phys. Rev. Lett.* **115**, 131601 (2015).
- [22] F. Brünner and A. Rebhan, Constraints on the  $\eta\eta'$  decay rate of a scalar glueball from gauge/gravity duality, *Phys. Rev. D* **92**, 121902 (2015).
- [23] F. Brünner, J. Leutgeb, and A. Rebhan, A broad pseudo-vector glueball from holographic QCD, *Phys. Lett. B* **788**, 431 (2019).
- [24] J. Leutgeb and A. Rebhan, Witten-Veneziano mechanism and pseudoscalar glueball-meson mixing in holographic QCD, *Phys. Rev. D* **101**, 014006 (2020).
- [25] F. Hechenberger, J. Leutgeb, and A. Rebhan, Radiative meson and glueball decays in the Witten-Sakai-Sugimoto model, *Phys. Rev. D* **107**, 114020 (2023).
- [26] T. Sakai and S. Sugimoto, Low energy hadron physics in holographic QCD, *Prog. Theor. Phys.* **113**, 843 (2005).
- [27] T. Sakai and S. Sugimoto, More on a holographic dual of QCD, *Prog. Theor. Phys.* **114**, 1083 (2005).
- [28] E. Witten, Anti-de Sitter space, thermal phase transition, and confinement in gauge theories, *Adv. Theor. Math. Phys.* **2**, 505 (1998).
- [29] N. R. Constable and R. C. Myers, Spin two glueballs, positive energy theorems and the AdS/CFT correspondence, *J. High Energy Phys.* **10** (1999) 037.
- [30] R. C. Brower, S. D. Mathur, and C.-I. Tan, Glueball spectrum for QCD from AdS supergravity duality, *Nucl. Phys.* **B587**, 249 (2000).
- [31] W.-S. Hou and A. Soni, Vector gluonium as a possible explanation for anomalous  $\psi$  decays, *Phys. Rev. Lett.* **50**, 569 (1983).
- [32] S. J. Brodsky, G. P. Lepage, and S. F. Tuan, Exclusive charmonium decays: The  $J/\psi(\psi') \rightarrow \rho\pi$ ,  $K^*\bar{K}$  puzzle, *Phys. Rev. Lett.* **59**, 621 (1987).
- [33] C.-T. Chan and W.-S. Hou, On the mixing amplitude of  $J/\psi$  and vector glueball  $O$ , *Nucl. Phys.* **A675**, 367C (2000).
- [34] X.-H. Mo, C.-Z. Yuan, and P. Wang, Study of the  $\rho - \pi$  puzzle in charmonium decays, *Chin. Phys. C* **31**, 686 (2007), <http://zgwlsc.xml-journal.net/en/article/id/d7f266c1-9574-470c-9a0d-c9da20a5a2e2>.
- [35] C. Ewerz, The Odderon in quantum chromodynamics, [arXiv:hep-ph/0306137](https://arxiv.org/abs/hep-ph/0306137).
- [36] V. M. Abazov *et al.* (D0, TOTEM Collaborations), Odderon exchange from elastic scattering differences between  $pp$

- and  $p\bar{p}$  data at 1.96 TeV and from pp forward scattering measurements, *Phys. Rev. Lett.* **127**, 062003 (2021).
- [37] R. C. Brower, M. Djuric, and C.-I. Tan, Odderon in gauge/string duality, *J. High Energy Phys.* **07** (2009) 063.
- [38] J. Polchinski, *String Theory: Volume 2, Superstring Theory and Beyond* (Cambridge University Press, Cambridge, England, 1998).
- [39] M. B. Green, J. A. Harvey, and G. W. Moore, I-brane inflow and anomalous couplings on D-branes, *Classical Quantum Gravity* **14**, 47 (1997).
- [40] G. S. Bali, F. Bursa, L. Castagnini, S. Collins, L. Del Debbio, B. Lucini, and M. Panero, Mesons in large-N QCD, *J. High Energy Phys.* **06** (2013) 071.
- [41] E. Witten, Current algebra theorems for the U(1) “Goldstone Boson”, *Nucl. Phys.* **B156**, 269 (1979).
- [42] G. Veneziano, U(1) without instantons, *Nucl. Phys.* **B159**, 213 (1979).
- [43] O. Aharony and D. Kutasov, Holographic duals of long open strings, *Phys. Rev. D* **78**, 026005 (2008).
- [44] K. Hashimoto, T. Hirayama, F.-L. Lin, and H.-U. Yee, Quark mass deformation of holographic massless QCD, *J. High Energy Phys.* **07** (2008) 089.
- [45] O. Bergman, S. Seki, and J. Sonnenschein, Quark mass and condensate in HQCD, *J. High Energy Phys.* **12** (2007) 037.
- [46] A. Dhar and P. Nag, Tachyon condensation and quark mass in modified Sakai-Sugimoto model, *Phys. Rev. D* **78**, 066021 (2008).
- [47] R. McNees, R. C. Myers, and A. Sinha, On quark masses in holographic QCD, *J. High Energy Phys.* **11** (2008) 056.
- [48] V. Niarchos, Hairpin-branes and tachyon-paperclips in holographic backgrounds, *Nucl. Phys.* **B841**, 268 (2010).
- [49] M. Suzuki, Strange axial-vector mesons, *Phys. Rev. D* **47**, 1252 (1993).
- [50] F. Divotgey, L. Olbrich, and F. Giacosa, Phenomenology of axial-vector and pseudovector mesons: Decays and mixing in the kaonic sector, *Eur. Phys. J. A* **49**, 135 (2013).
- [51] B. A. Burrington, V. S. Kaplunovsky, and J. Sonnenschein, Localized backreacted flavor branes in holographic QCD, *J. High Energy Phys.* **02** (2008) 001.
- [52] F. Bigazzi and A. L. Cotrone, Holographic QCD with dynamical flavors, *J. High Energy Phys.* **01** (2015) 104.
- [53] S. K. Domokos and N. Mann, Glueball-meson mixing in holographic QCD, *J. High Energy Phys.* **06** (2022) 029.
- [54] A. Tomasiello, *Geometry of String Theory Compactifications* (Cambridge University Press, Cambridge, England, 2022), p. 1.
- [55] E. Bergshoeff, R. Kallosh, T. Ortin, D. Roest, and A. Van Proeyen, New formulations of D = 10 supersymmetry and D8—O8 domain walls, *Classical Quantum Gravity* **18**, 3359 (2001).
- [56] F. Giacosa, J. Sammet, and S. Janowski, Decays of the vector glueball, *Phys. Rev. D* **95**, 114004 (2017).
- [57] D. Parganlija, P. Kovacs, G. Wolf, F. Giacosa, and D. H. Rischke, Meson vacuum phenomenology in a three-flavor linear sigma model with (axial-)vector mesons, *Phys. Rev. D* **87**, 014011 (2013).
- [58] W. I. Eshraim, S. Janowski, F. Giacosa, and D. H. Rischke, Decay of the pseudoscalar glueball into scalar and pseudoscalar mesons, *Phys. Rev. D* **87**, 054036 (2013).
- [59] W. I. Eshraim and S. Schramm, Decay modes of the excited pseudoscalar glueball, *Phys. Rev. D* **95**, 014028 (2017).
- [60] Y.-Q. Chen and E. Braaten, An explanation for the  $\rho - \pi$  puzzle of  $J/\psi$  and  $\psi'$  decays, *Phys. Rev. Lett.* **80**, 5060 (1998).
- [61] P. G. O. Freund and Y. Nambu, Dynamics in the Zweig-Iizuka rule and a new vector meson below 2 GeV/ $c^2$ , *Phys. Rev. Lett.* **34**, 1645 (1975).
- [62] G. W. S. Hou, (Vector) glueballs and charmonium decay revisited, [arXiv:hep-ph/9609363](https://arxiv.org/abs/hep-ph/9609363).
- [63] G. W.-S. Hou, The case for a vector glueball, [arXiv:hep-ph/9707526](https://arxiv.org/abs/hep-ph/9707526).
- [64] R. L. Workman (Particle Data Group), Review of particle physics, *Prog. Theor. Exp. Phys.* **2022**, 083C01 (2022).
- [65] J. P. Lees *et al.* (BABAR Collaboration), Study of the reactions  $e^+e^- \rightarrow K^+K^-\pi^0\pi^0\pi^0$ ,  $e^+e^- \rightarrow K_S^0K^\pm\pi^\mp\pi^0\pi^0$ , and  $e^+e^- \rightarrow K_S^0K^\pm\pi^\mp\pi^+\pi^-$  at center-of-mass energies from threshold to 4.5 GeV using initial-state radiation, *Phys. Rev. D* **107**, 072001 (2023).
- [66] F. Hechenberger, K. A. Mamo, and I. Zahed, preceding paper, Threshold photoproduction of  $\eta_c$  and  $\eta_b$  using holographic QCD, *Phys. Rev. D* **109**, 074013 (2024).